A computational acumen into the relative applicability of geometrical and quantum chemical criteria in assessing intramolecular hydrogen bonding (IMHB) interaction: 5-Halosalicylic…

ARTICLE *in* COMPUTATIONAL AND THEORETICAL CHEMISTRY · JUNE 2013

Impact Factor: 1.55 · DOI: 10.1016/j.comptc.2013.06.017

4 AUTHORS, INCLUDING:

Aniruddha Ganguly
University of Calcutta
19 PUBLICATIONS **67** CITATIONS
SEE PROFILE

Bijan Kumar Paul
Indian Institute of Science Education and R…
72 PUBLICATIONS **895** CITATIONS
SEE PROFILE

Computational and Theoretical Chemistry 1018 (2013) 102–114

Contents lists available at SciVerse ScienceDirect

Computational and Theoretical Chemistry

journal homepage: www.elsevier.com/locate/comptc

A computational acumen into the relative applicability of geometrical and quantum chemical criteria in assessing intramolecular hydrogen bonding (IMHB) interaction: 5-Halosalicylic acids as representative examples

Aniruddha Ganguly [2], Bijan Kumar Paul [1,2], Soumen Ghosh, Nikhil Guchhait *

Department of Chemistry, University of Calcutta, 92 A.P.C. Road, Calcutta 700 009, India

ARTICLE INFO

Article history:
Received 1 May 2013
Received in revised form 17 June 2013
Accepted 17 June 2013
Available online 26 June 2013

Keywords:
Density functional theory
Intramolecular hydrogen bonding
Atoms-In-Molecule
Natural Bond Orbital
Molecular electrostatic potential
Resonance assisted hydrogen bond

ABSTRACT

Density functional theory (DFT) based computational study has been performed to characterize intramolecular hydrogen bonding (IMHB) interaction in a series of salicylic acid derivatives having different halogen substitution at the 5-position on the benzene ring. The molecular systems studied are salicylic acid (SA), 5-fluorosalicylic acid (5FSA), 5-chlorosalicylic acid (5ClSA) and 5-bromosalicylic acid (5BrSA). Particular emphasis has been given on the analysis of IMHB interaction by the calculation of electron density $\rho(\mathbf{r})$ and Laplacian $\nabla^2\rho(\mathbf{r})$ at the bond critical point using Atoms-In-Molecule (AIM) theory. Topological features and energy densities based on $\rho(\mathbf{r})$ through the perturbation of the IMHB distances suggest that at equilibrium geometry the IMHB interaction develops certain characteristics typical of a covalent interaction. Concomitantly, the role of charge transfer interaction in the IMHB has been critically addressed under the provision of Natural Bond Orbital (NBO) analysis. The formation of Resonance Assisted Hydrogen Bond (RAHB) in the studied molecular systems is also delineated from quantum chemical calculations. The interplay between aromaticity and RAHB is discussed in this context using both geometrical and magnetic criteria as the aromaticity descriptors. The optimized geometry features, analysis of the molecular electrostatic potential map have also been found to produce a consensus view in relation with the formation of RAHB in the studied systems. The lack of a specific pattern of IMHB energy in the studied molecules with the electronegativity of the substituent has also been attempted to address critically. Another major aspect of the present study is the argument about the superiority of quantum chemical criteria over geometrical criteria for the assessment of IMHB interaction in the studied compounds.

1. Introduction

The hydrogen bond is omnipresent in nature and indisputably the most important 'weak' interaction encountered in the natural system to sustain and maintain life-cycle on this planet [1–4]. It plays a dual role in biological systems; on one hand, in the form of a collectively strong directional interaction it leads to stable supramolecular architectures which are inevitable for the construction of fundamental building blocks of life, and on the other, by virtue of its dynamic features, it serves as an active site for the occurrence of a vista of interactions [4,5]. Hydrogen bonding (HB) plays crucial roles in defining the crystal packing of many organic and organometallic molecules and is the source of specific properties of associated liquids like water and thus crops up as a demanding topic of research [4–8].

The classical hydrogen bonds correspond to those formed by two heteroatoms, X and Y (which have already saturated valencies), with a hydrogen atom bonded to one of them and located approximately in between (X—H···Y). Primarily, H-bonding has been considered as an electrostatic attraction between the positive end of the bond dipole of X—H and the center of negative charge on Y (generally a lone pair of electrons) [9–11]. Unlike typical chemical bonds, the H-bond ranges over a large scale of energy, from very weak ones to very strong ones depending upon the corresponding groups involved [4,12–14]. One particular type of H-bonding interaction is the one found in association with excited state intramolecular proton transfer (ESIPT) reaction, i.e., the intramolecular hydrogen bond (IMHB) which is a particular case of the interaction occurring within the same molecular architecture. The IMHB interaction is well-documented to have its crucial impact on the feasibility and rate of ESIPT process [15–17]. Ever since the pioneering

* Corresponding author. Tel.: +91 3323508386; fax: +91 3323519755.
E-mail address: nguchhait@yahoo.com (N. Guchhait).
[1] Present address: Department of Chemistry and Biochemistry, University of Colorado, Boulder, CO 80309, United States.
[2] These authors contributed equally to this work.

2210-271X/$ - see front matter © 2013 Elsevier B.V. All rights reserved.
http://dx.doi.org/10.1016/j.comptc.2013.06.017

work of Weller [18], the ESIPT phenomenon has led to prospective opportunities for both fundamental and applicative research in photochemical and photobiological arenas due to the potential utility of the corresponding molecules to probe many biological, biomimicking and supramolecular assemblies as well as to serve as photostabilizers, UV absorbers and so forth [19–22]. Salicylic acid (SA) and its derivatives are typical candidates for the study of ESIPT reactions. Although several attempts have been made to study the substitution effect on ESIPT of SA, those are mainly focused on substitution at the IMHB ring site [23–25]. Studies intending to delve into the effects of substitution on the adjoined aromatic nucleus have, rather, been sporadically addressed [26,27]. Following the aforesaid point, in this present contribution, we have focused on a thorough exploration of the effect of electronegative substituent on the aromatic ring in a series of molecular systems *viz.*, SA, 5-fluorosalicylic acid (5FSA), 5-chlorosalicylic acid (5ClSA) and 5-bromosalicylic acid (5BrSA) from computational perspectives. Particular emphasis has been rendered on the application of different quantum chemical tools for detection and evaluation of the IMHB interaction in the studied molecules. The topological properties of IMHB interaction are assayed under the provision of Atoms-In-Molecule (AIM) [32,33] methodology, while a critical evaluation of the role of hyperconjugativen charge transfer interaction is deduced from the Natural Bond Orbital (NBO) population analysis [34,35]. The possibility for the Resonance Assisted Hydrogen Bond (RAHB) interaction [36] is also scrutinized from geometrical criteria as well as quantum chemical analysis. Further, the interplay between aromaticity and RAHB has been explored in this context. Finally, the geometrical and quantum chemical criteria have been directly compared in an endeavor to provide a picture arguing the origin of and then to find reliable criteria for evaluation of H-bond strength.

2. Computational procedures

2.1. Geometry optimization

The structural calculations have been performed on Gaussian 03W suite of programs [37]. The ground-state structure for various possible low energy conformations of 5-halosalicylic acid (5XSA) have been computed at the Density Functional Theory (DFT) level [38] using B3LYP hybrid functional (which comprises of Becke's three-parameter hybrid exchange functional and the nonlocal correlation functional of Lee, Yang, and Parr) [39,40]. For this purpose 6-311++G(d,p) basis set has been chosen because this basis set is of triple-ζ quality for valence electrons with diffuse functions which are useful in calculations for anions and structures with lone pair electrons [31,41]. The characteristic of local minimum corresponding to the optimized geometries has been verified by establishing that matrices of energy second derivatives (Hessian) have no imaginary frequency [16,17,31].

2.2. NBO and AIM calculations

The Natural Bond Orbital (NBO) analysis has been employed to evaluate the direction and magnitude of donor–acceptor interactions. The necessary computations for NBO analysis [35] has been performed on Gaussian 03W software package [37]. The contour plot for visualization of the NBO result is constructed on NBO View (Version 1.1) software package using the standard keywords implemented therein. Similarly, the AIM [32,33] calculation has also been performed on Gaussian 03W software at B3LYP/6-31G(d,p) level using the standard keywords implemented therein.

2.3. Calculation of aromaticity indices

The Harmonic Oscillator Model of Aromaticity (HOMA) [42] index has been employed as a geometrical criterion of local aromaticity. According to the definition proposed by Kruszewski and Krygowski [42] the applied formula is as follows:

$$HOMA = 1 - \frac{1}{n}\sum_{j=1}^{n}\alpha_i(R_{opt,i} - R_j)^2 \quad (1)$$

where n corresponds to the number of bonds within the analyzed ring. The term α being a normalization constant fitted to give a value of HOMA = 1 for ideally aromatic systems with all bond lengths equal to optimal value, R_{opt}, and HOMA = 0 for an ideally nonaromatic species (for CC bonds: $\alpha_{C-C} = 257.7$ and $R_{opt,CC} = 1.388$ Å). The greater the magnitude of the HOMA index, the more aromatic is the ring under investigation and hence conforming to greater extent of delocalization of the π-electrons of the system.

As proposed by Schleyer et al. the Nucleus Independent Chemical Shift (NICS) index has been used as a magnetic indicator of local aromaticity [43]. For the NICS calculations, we have adopted the gauge-independent atomic orbital (GIAO) formalism using the "Bq" probe atom to designate the positions for evaluation [43,44]. NICS(0) is defined as the negative value of the absolute shielding computed at a ring center determined by the nonweighted average of the heavy atoms' coordinates in the ring. Rings with large negative NICS(0) values are considered aromatic. The more negative the NICS(0) value, the more aromatic the ring is [43,44]. It has been shown by Lazzeretti and Aihara [45,46] the NICS(0) values may contain significant spurious contributions from the in-plane tensor components arising from σ-bonding that are not related to aromaticity. So, to complement the NICS analysis, NICS(1) values have also been calculated as the negative values of absolute shielding measured at 1 Å above the center of the ring which has been postulated to better reflect the aromaticity patterns because at 1 Å the effects of the π-electron ring current are dominant and local σ-bonding contributions are diminished [44–46].

3. Results and discussions

3.1. Geometrical criteria for assessing the presence of IMHB interaction in 5XSA (X = H, F, Cl, Br)

An idea of the presence of intramolecular hydrogen bonding (IMHB) interaction in the studied molecular systems, *viz.*, SA, 5FSA, 5ClSA and 5BrSA is assessed from the comparison of the optimized geometrical parameters of the closed conformers (i.e., C-forms) with those in the respective open counterparts (O-forms, *vide* Scheme 1). Since the open forms of the molecules are devoid of IMHB interaction, a comparison of their geometrical parameters with those of the corresponding closed forms will reflect the modifications in optimized geometrical parameters as imparted by the presence of IMHB. As seen in Table 1a, the lengthening of the proton donating bond (H_1—O_d distance) in the closed form compared to that in the open form is in consensus with the occurrence of IMHB interaction in all the molecular systems under investigation [1,2,16,17,31]. Apart from this, the data compiled in Table 1a also reveal some discernible modulations in geometry parameters surrounding the entire IMHB site in the studied molecules, e.g., lengthening of C_4═O_a and C_2═C_3 bonds along with shortening of C_3—C_4 and O_d—C_2 distances in the closed form (with respect to that in open form, *vide* Scheme 1). The changes in the geometry parameters in these directions upon moving from the closed to the open form can be corroborated to the presence of resonance assistance in the IMHB interaction present in the studied molecular systems [1,2,16,17,31]. It is, however, noted that in spite of the general

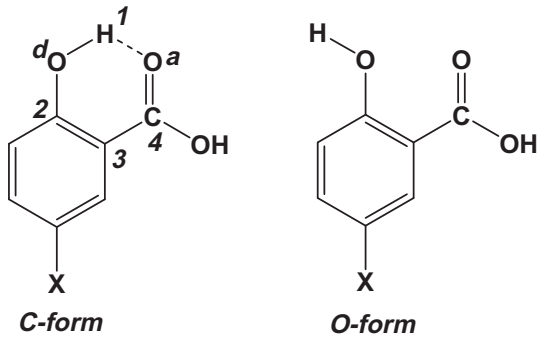

X = H: Salicylic acid (SA),
X = F: 5-Fluorosalicylic acid (5FSA),
X = Cl: 5-Chlorosalicylic acid (5ClSA),
X = Br: 5-Bromosalicylic acid (5BrSA)

Scheme 1. Schematic molecular structures of the molecular systems under investigation. The intramoleclar hydrogen bonded closed form (C-form) and the non-hydrogen bonded open form (O-form) are shown along with the numbering of atoms used throughout the study.

trend in the variation of the optimized geometry parameters on moving from closed to the open form of the molecules, no clear trend is observed as a function of electronegativity of the substituent at the 5-position on the aromatic nucleus.

In this context, endeavors are made toward evaluation of verisimilar estimates for the energy of the IMHB interactions in the molecular systems under study. This attempt is, however, fraught with ambiguities in the literature given the lack of any unequivocally accepted approach as against the intermolecular hydrogen bonding case. Such tailback has eventually led to the proposition of various approaches in the literature to estimate the energy of an intramolecular hydrogen bond; the methods adopted in the present work are outlined below:

(1) *Closed vs. open form*: In this approach the energy of the IMHB is approximated to the energy difference between the intramolecularly hydrogen bonded closed form and the open form (Scheme 1) in which the hydrogen donor —OH group is rotated 180° apart from the hydrogen bonded configuration to generate the non-hydrogen bonded open form [47]:

$$\text{Hydrogen bond energy, } E_{HB}^{(1)} = \Delta E = E_{\text{closed}} - E_{\text{open}} \tag{2}$$

This approach, however, comprises the intrinsic assumption of ignoring the influence of the aforementioned rotation on overall geometry parameters of the concerned molecule other than simply cleavage of the hydrogen bond from the contiguous IMHB circuit.

(2) *Empirical energy-geometry correlations*: Establishing the correlation between energetic properties and geometry parameters within IMHB frameworks has remained a concern on the vanguard of research on the topic. The one that has been widely accepted till date appears to be the proposition by Musin and Mariam [48] which suggests an exponential correlation as follows:

$$E_{\text{HB}}^{(2)} = (-5.554 \times 10^5)\exp(-4.12 \times R_{\text{O}\cdots\text{O}}) \tag{3}$$

in which $R_{\text{O}\cdots\text{O}}$ represents the distance between the O_d and O_a atoms in the equilibrium geometry in Å (*cf.* Scheme 1). The negative sign before E_{HB} has been introduced to maintain the consistency in the use of notation throughout the work, *cf.* in Ref. [48], the hydrogen bond energy is denoted as a negative number while in the present work it is denoted as a positive number.

(3) *Conformational analysis*: This method accounts for the IMHB energy in a given molecular system from a complex conformational analysis of the four possible conformers, *viz.*, ZZ, EZ, ZE and EE, emanating from rotation of the donor and acceptor functional moieties [49]. The ZZ conformer represents the lowest energy intramolecularly hydrogen bonded closed conformer (*vide* Scheme 1), EZ and ZE conformers are obtained by rotating respectively the donor and acceptor groups across their respective carbon–carbon linkages and the EE conformer designates the fictitious conformer in which both the donor and the acceptor groups have been rotated about their bonds. Following the scheme used in the literature [49] the hydrogen bond energy is assayed as:

$$E_{\text{HB}}^{(3)} = \frac{1}{2}(E_{\text{EZ}}^{f} + E_{\text{EE}}^{f}) - E_{ZZ} \tag{4}$$

In this equation, $E_{\text{EZ}}^{f}(E_{\text{EE}}^{f})$ designates the energy of the fictitious EZ (EE) conformer in which the bond lengths are the same as in the ZZ conformer whose energy is given by E_{ZZ} in its equilibrium configuration.

(4) *Local potential energy density*: In this method, the IMHB energy is connected to the local potential energy density at the hydrogen bond critical point (V_{CP}) and the atomic volume element (a_0^3) through the following equation [50]:

Table 1
(a) Differences in selective optimized geometry parameters (B3LYP/6-311++G(d,p)) at the IMHB framework between the closed form and the open form of the studied molecular systems ($\Delta = R_{\text{Closed}} - R_{\text{Open}}$ in Å, atom numbering according to Scheme 1) (b). Calculated estimate of IMHB energies (E_{HB} in kcal mol^{-1}) for the studied molecular systems following different methods (*cf.* Section 3.1).

Geometry parameters	SA	5FSA	5ClSA	5BrSA
(a) Comparison of optimized geometry parameters between closed and open forms				
$\Delta(C_4{=}O_a)$	0.0199	0.0194	0.0196	0.0195
$\Delta(H_1{-}O_d)$	0.0177	0.0172	0.0176	0.0175
$\Delta(O_d{-}C_2)$	−0.0117	−0.0118	−0.0117	−0.0116
$\Delta(C_2{=}C_3)$	0.0052	0.0038	0.0043	0.0040
$\Delta(C_3{-}C_4)$	−0.0211	−0.0213	−0.0213	−0.0213
$\Delta(O_d{-}O_a)$	−0.0822	−0.0773	−0.0805	−0.0778
(b) Calculated IMHB energies by different methods				
Molecule	$E_{HB}^{(1)}$	$E_{HB}^{(2)}$	$E_{HB}^{(3)}$	$E_{HB}^{(4)}$
SA	11.13	11.14	10.95	12.14
5FSA	11.07	10.97	10.89	11.83
5ClSA	11.08	11.12	10.76	11.58
5BrSA	11.10	11.06	10.94	11.92

$$E_{HB}^{(4)} = -\frac{a_0^3}{2} V_{CP} \quad (5)$$

A comparative view of the IMHB energy estimates as computed from the aforementioned methods is displayed in Table 1b.

3.2. Simulated infrared (IR) spectra to analyze the presence and strength of IMHB in 5XSA (X = H, F, Cl, Br)

IR spectroscopy has long been recognized as a rewarding tool for characterizing the presence and assessing the strength of H-bond present in a molecule. Herein, we have exploited this strategy to rationalize the presence of IMHB in the studied systems, and the corresponding data are summarized in Table 2. Typically, the formation of IMHB in a molecule is characterized *via* a hyperconjugative charge transfer from the lone pair of the acceptor atom (in the present case, O_a) to the σ^* orbital of the donor bond (O_d—H_1), which is essentially accompanied with some decrement in the O_d—H_1 bond order as reflected in weakening of the O_d—H_1 bond energy in the closed form as compared to that in the open form and thereby accounts for the observed shift in the corresponding IR stretching frequency (*vide* Table 2) [2,31,51], e.g., the O_d—H_1 IR stretching frequency, on moving from the H-bonded closed form to the open form, undergoes blue-shifts of $\sim$340 cm^{-1} for all the four compounds studied (*vide* Table 2), advocating for the presence of IMHB interactions therein (having comparable H-bonding energy) as well as inferring that there is no or minute effect of the electronegativity of the 5-halo substituent on the formed H-bonds. As apparent from Table 2, the theoretical stretching frequencies of all the studied compounds correspond reasonably well with the respective experimentally observed frequencies [31,51,52].

3.3. Topological analysis: Atoms-In-Molecule (AIM) study

Atoms-In-Molecule (AIM) method of Bader [32], which is mainly based on an analysis of electron density at specific points ($\rho(\mathbf{r})$), provides an effective measure of detection as well as characterization of H-bonding [16,17,32,33,53]. On the basis of this theory, Koch and Popelier has proposed a few criteria relying on the electron density parameter $\rho(\mathbf{r})$, to detect the presence of hydrogen bond [54–56]. According to them, the existence of a hydrogen bond is characterized by (i) the presence of a bond critical point (BCP) between the hydrogen atom and the acceptor atom; (ii) the value of $\rho(\mathbf{r})$ at this BCP (ρ_c) lies within the range [0.002, 0.040] a.u.; (iii) the Laplacian of $\rho(\mathbf{r})$ at this BCP ($\nabla^2\rho_c$) is positive and the corresponding value is within the range [0.02, 0.15] a.u.; and (iv) the hydrogen atom and the acceptor atom must mutually penetrate i.e., the bonded radius of the hydrogen atom and the acceptor atom must each be smaller than the corresponding nonbonded (van der Waals') radii [16,17,54–56].

However, recent time has witnessed flourishing extension of the AIM methodology including some other parameters like electronic energy densities and bond ellipticity [13,31,54]. Though in general AIM studies deal only with equilibrium geometries, we have extended it by exploring the evolution of the molecular geometries over a range of intramolecular hydrogen bond (HB) distances [16,17,53] to acquire a more elaborative description of the hydrogen bonding interaction scenario within the presently investigated molecular systems. In this work, the wave functions of H-bonded molecular geometries obtained from 6-31G(d,p) level of calculation has been employed to characterize the topological properties [57].

Table 2
Summary of the simulated IR spectroscopic data for SA, 5FSA, 5ClSA, and 5BrSA (DFT/B3LYP/6-311++G(d,p)).

Molecule	ν_C[a] (cm^{-1})	ν_O[b] (cm^{-1})	$\Delta\nu$[c] (cm^{-1})	ν_{Expt}[d] (cm^{-1})
SA	3473	3819	−346	3236
5FSA	3487	3823	−336	3244
5ClSA	3476	3820	−344	3233
5BrSA	3477	3819	−342	3246

[a] ν_C designates the calculated O_d—H_1 stretching frequency in the closed form.
[b] ν_O designates the calculated O_d—H_1 stretching frequency in the open form.
[c] $\Delta\nu = \nu_C - \nu_O$.
[d] Experimentally obtained O_d—H_1 stretching frequency as obtained from IR spectra of the respective compounds.

3.3.1. Electron density at the bond critical point (BCP) and ring critical point (RCP)

According to Bader's theory, identification of a critical point (CP) and the existence of a bond path in equilibrium geometry are necessary and sufficient conditions for assigning the presence of a bond between two atoms [57,58]. However, Cioslowski et al. have claimed that it should be interpreted as attractive or repulsive interactions leading to either bonding or nonbonding situation [59,60], which was further validated by Bickelhaupt and coworkers [61,62]. These arguments in turn reveal that care must be taken during interpretation of the AIM topological parameters which has hence been a prime concern in the present study [59–65]. Fig. 1 displays the variation of ρ_c ($\rho(\mathbf{r})$ at BCP) and its Laplacian $\nabla^2\rho_c$ ($\nabla^2\rho(\mathbf{r})$ at BCP) as a function of $H_1\cdots O_a$ IMHB distance for the studied molecular systems. The relevant AIM topological parameters corresponding to the respective optimized geometries are summarized in Table 3 which shows that ρ_c i.e., $\rho(\mathbf{r})$ at the BCP for the ground state optimized geometry has a value close to 0.040 a.u. (the maximum Popelier threshold value) for all the studied molecules [55,56], which justifies the presence of intramolecular hydrogen bond in the studied molecules. From the figure, the steep variations in magnitude of the AIM topological parameters (ρ_c and $\nabla^2\rho_c$) as a function of $H_1\cdots O_a$ IMHB distance are noteworthy. Such notable decrease of these parameters with increasing $H_1\cdots O_a$ bond length from the equilibrium value advocates for the presence of strong hydrogen bonding interaction in the studied molecular systems and is believed to be the result of decrease in extent of orbital overlap with elongation of the $H_1\cdots O_a$ bond length [16,17,53,55,56]. It is interesting to note in the present context that ρ_c corresponding to the optimized geometry for all the molecular systems is slightly greater than the maximum Popelier threshold value of 0.040 a.u. [56]. On the basis of Bader's theory, this can be treated as a hint for the presence of partial covalency in the concerned IMHB interactions [32,33]. This observation thus again points towards the presence of resonance assistance in the IMHB interactions and is further assessed in forthcoming discussions.

Also the existence of ring critical points (RCPs; *vide* Table 3) within the quasi-rings formed by the hydrogen bonded network in the optimized geometries of the studied molecules (*vide* Scheme 1) manifest the presence of IMHB interaction in the molecular systems [54,58]. The variation of AIM topological parameter $\rho(\mathbf{r})$ at RCP as a function of $H_1\cdots O_a$ IMHB distance for all the studied compounds are pictorially presented in Fig. 2. A similar trend of variation of $\rho(\mathbf{r})$ at RCP as compared to that in case of $\rho(\mathbf{r})$ at BCP with increasing $H_1\cdots O_a$ bond length suggests the presence of strong hydrogen bonding interaction in the studied molecular systems [54,58,63–65] and yet again no apparent trend is observed as a function of the electronegativity of the 5-substituent.

3.3.2. Electronic energy density

The local energy densities computed at the BCPs yield valuable information to rationalize the nature of an interaction. From quantum mechanical point of view, the local potential energy density $V(\mathbf{r})$ can be obtained from the Virial equation expressed as follows [31,43,53,54,66]:

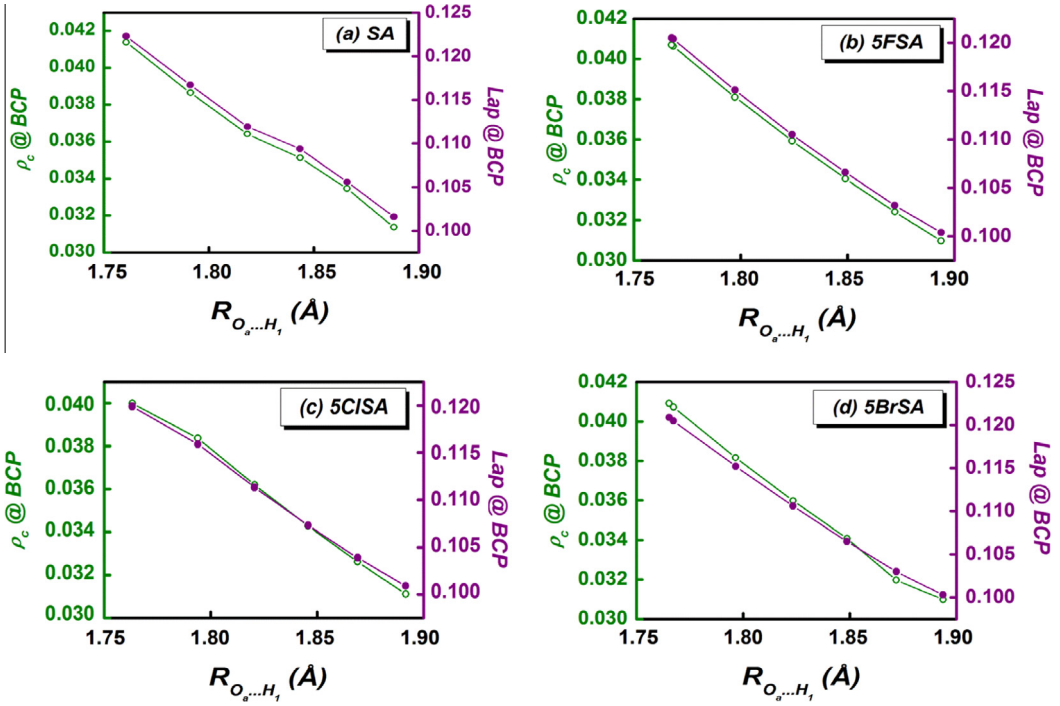

Fig. 1. Plot of variation of ρ_c ($\rho(\mathbf{r})$ at BCP) (–○–) and $\nabla^2\rho_c$ ($\nabla^2\rho(\mathbf{r})$ at BCP) (–●–) as a function of the IMHB distance ($O_a\cdots H_1$) for the C-form of (a) SA, (b) 5FSA, (c) 5ClSA and (d) 5BrSA. The solid lines only provide a visual guide to the pattern of variation.

Table 3
Summary of the AIM topological parameters at the Bond and Ring Critical Points (BCP and RCP) of the IMHB corresponding to the optimized geometry of the studied molecular systems.

Molecule	ρ_c (a.u.)	$\nabla^2\rho_c$ (a.u.)	$\rho_{(RCP)}$ (a.u.)	G_c[a] (a.u.)	V_c[a] (a.u.)	H_c[a] (a.u.)
SA	0.0414	0.1223	0.0175	0.0346	−0.0387	−0.0040
5FSA	0.0407	0.1205	0.0174	0.0339	−0.0377	−0.0038
5ClSA	0.0406	0.1199	0.0173	0.0334	−0.0369	−0.0035
5BrSA	0.0409	0.1209	0.0174	0.0341	−0.0380	−0.0039

[a] 1 a.u. of energy density = 1.77178×10^{34} kJ mol^{-1} m^{-3}.

$$V(\mathbf{r}) + 2G(\mathbf{r}) = \frac{1}{4}\nabla^2\rho(\mathbf{r}) \tag{6}$$

where $G(\mathbf{r})$ and $V(\mathbf{r})$ are respectively the electronic kinetic and potential energy densities. Since $G(\mathbf{r}) \rangle 0$ and $V(\mathbf{r}) \langle 0$, the sign of the Laplacian at the BCP determines which energy density dominates at **r**. Now, the total energy density, $H(\mathbf{r}) = V(\mathbf{r}) + G(\mathbf{r})$ at the BCP, (i.e., $H_c = V_c + G_c$), characterizes the type of bond and is often invoked to be a more reliable parameter than the Laplacian [54]. A negative H_c reflects the dominance of V which according to equation 6 may be assumed as a consequence of accumulation of charge at the BCP [31,43,53,54]. Therefore, in bonds with any degree of covalency the following condition will hold: $|V_c| \rangle G_c$ and $H_c \langle 0$. However, bonds in which this condition is satisfied but $|V_c| \langle 2G_c$ will be characterized by $\nabla^2\rho_c \rangle 0$ implying a closed-shell interaction, while $H_c \langle 0$ would suggest a shared interaction. This type of interaction is described to be partially covalent and partially electrostatic [31,43,53,54].

Fig. 3 displays the energetic properties of BCP as a function of IMHB distance in the studied molecules and it is apparent that both $V(\mathbf{r})$ and $G(\mathbf{r})$ are well correlated to the presence of hydrogen bonding interaction. The results in Table 2 show a positive value for the Laplacian of electron density for all the studied molecules conforming to a closed shell interaction. However, a slightly negative value of $H(\mathbf{r})$ at the BCP (i.e., H_c) implies the presence of partial covalency. This finding reinforces the aforementioned observation with $\rho(\mathbf{r})$ at BCP.

3.3.3. Bond ellipticity

The ellipticity parameter (ε) at the BCP can be interpreted as a measure of the anisotropy of the curvature of the electron density in the directions perpendicular to the bond, in which a zero value signatures the absence of anisotropy. Thus ellipticity is often regarded as a sensitive index to monitor the π-character of bonds. The ellipticity at the BCP is a direct measure of the degree to which the electron density is unequally distorted in perpendicular directions away from the bond axis [32]. From *ab initio* studies, Bader and co workers have calculated the ellipticities of the C—C bonds in ethane, benzene, and ethylene to be 0.0, 0.23, and 0.45 which correspond to pure single, partially double, and pure double bonds, respectively. Deviations from those values of bond ellipticities faithfully recover the anticipated consequences of the conjugation and hyperconjugation models of electron delocalization [32,33].

The corresponding bond ellipticity parameters obtained using AIM calculation for the compounds under investigation are summarized in Table 4. As expected, both the O_d—H_1 and $O_a\cdots H_1$ bonds show an ellipticity value close to 0.0, indicating the presence of single bonds at the corresponding sites. Interestingly, for all the other associated bonds at the IMHB site ellipticity values vary in the range ~0.1–0.24 which in turn advocates for the notion of the absence of pure single and pure double bond characters across the bonds concerned and hence corroborate to the π-electron delocalization concept relating to resonance-assisted hydrogen bonds.

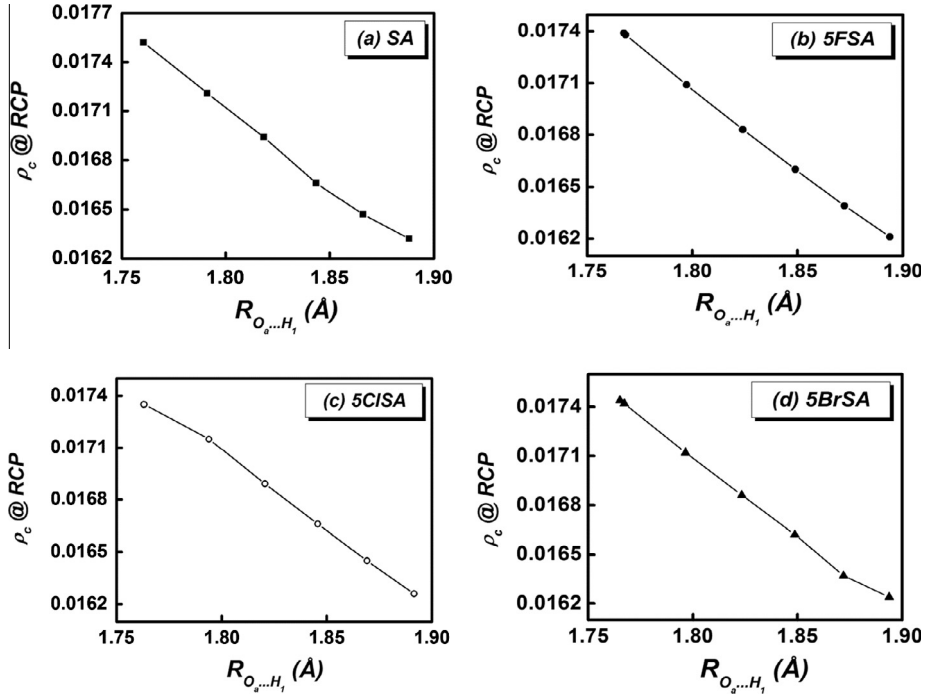

Fig. 2. Plot of variation of ρ_c ($\rho(\mathbf{r})$ at RCP) as a function of the IMHB distance ($O_a\cdots H_1$) for the C-form of (a) SA (–■–), (b) 5FSA (–●–), (c) 5ClSA (–○–) and (d) 5BrSA (–▲–). The solid lines only provide a visual guide to the pattern of variation.

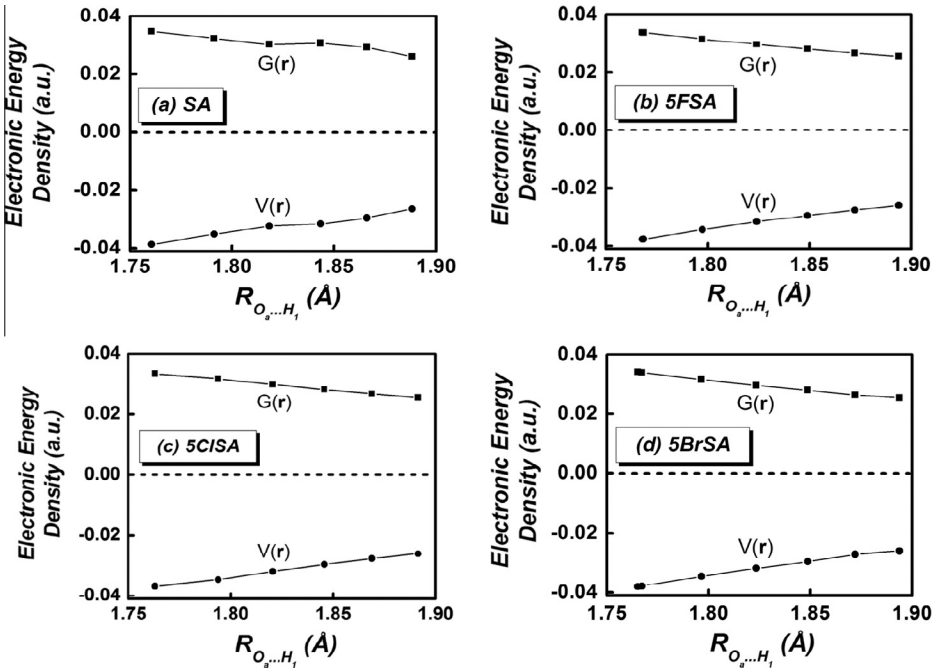

Fig. 3. Relationship between the electronic energy density properties (G(r) (–■–) and V(r) (–●–)) of BCP and the intramolecular H-bond distance ($O_a\cdots H_1$) in (a) SA, (b) 5FSA, (c) 5ClSA and (d) 5BrSA. The solid lines only provide a visual guide to the pattern of variation.

3.4. Population analysis: Natural Bond Orbital (NBO) study

The Natural Bond Orbital (NBO) method, proposed by Weinhold et al. has been recognized as a potential tool for the rationalization of H-bonds, which correlates well with the changes in bond length in accordance with basic chemical concepts. It is also used to gain information on the changes of charge densities at the proton donor and acceptor as well as in the bonding and antibonding orbitals. Now, the interaction between filled (e.g., the lone-pair) and antibonding orbitals represents the deviation of the molecule from the Lewis structure and can be used as a measure of the delocalization due to the presence of hydrogen bonding interaction [34,35]. Hydrogen bonds, within the NBO framework, are conventionally interpreted to be formed as a result of charge transfer from the proton acceptor to the proton donor, and hence the amount of charge transfer plays a significant role in determining the

Table 4
Ellipticity (ε) parameters at the BCPs of the bonds involved in resonance-assisted hydrogen bond formation in the studied molecular systems (atom numbering according to Scheme 1).

Bond	Ellipticity (ε)			
	SA	5FSA	5ClSA	5BrSA
O_d—H_1	0.0177	0.0179	0.0176	0.0175
C_2=C_3	0.2328	0.2416	0.2356	0.2350
C_3—C_4	0.1618	0.1593	0.1584	0.1582
C_4=O_a	0.1014	0.1034	0.1032	0.1031
O_a···H_1	0.00243	0.00322	0.00320	0.00358

elongation or contraction of the H···Y bond (considering the hydrogen bonded system X—H···Y). For each donor and acceptor, the stabilization energy ΔE_2 associated with an i–j delocalization is calculated using the following equation [31,34,35]:

$$\Delta E_2 = \Delta E_{ij}^{(2)} = \frac{\left|\left\langle \Phi_i|\hat{F}|\Phi_j\right\rangle\right|^2}{(\varepsilon_i - \varepsilon_j)} \quad (7)$$

where $\hat{F}$ is the Fock operator and ε_i and ε_j correspond to the energy eigenvalues of the donor NBO, Φ_i, and the acceptor NBO, Φ_j, respectively.

The results of NBO analysis on the studied molecular systems are depicted in Fig. 4 which reveals that the hyperconjugative charge transfer stabilization energy (ΔE_2) from O_a lone pair (LP2) to the $\sigma^*(O_d$—$H_1)$ orbital is sharply diminished with elongation of the O_a···H_1 IMHB distance, justifying the presence of IMHB interaction in the molecules. This is again substantiated from the contour plot showing the overlap between the O_a lone pair orbital and the $\sigma^*(O_d$—$H_1)$ orbital (Fig. 5). The presence of a finite, nonzero overlap between the orbitals obviously manifests the presence of a nonzero stabilization interaction (ΔE_2) due to the hyperconjugative charge transfer interaction from O_a lone pair to the σ^* orbital of the O_d—H_1 bond resulting in the formation of the IMHB interaction. Also a good extent of overlap stands in favor of a strong IMHB in the studied molecular systems, in corroboration to other findings discussed above. However, it is also seen in Fig. 4 that the variation of LP1 → $\sigma^*(O_d$—$H_1)$ hyperconjugative charge transfer interaction is much less sensitive to the O_a···H_1 distance and is almost parallel to the ordinate axis. Such scenario can be visualized as a manifestation of the directional nature of hydrogen bonding. Of the two lone pairs (LP1 and LP2) of O_a atom, one is properly oriented along the direction of the H_1···O_a H-bond axis so as to ensure a substantial LP2 → $\sigma^*(O_d$—$H_1)$ hyperconjugative charge transfer interaction leading to the formation of the IMHB. Whereas, the other lone pair (LP1) is not properly oriented to undergo such interaction. The variation of population (occupation number as calculated from NBO analysis) of $\sigma^*(O_d$—$H_1)$ as well as of LP2 (O_a) as a function of IMHB distance (O_a···H_1) is also found to be in accordance with the occurrence of IMHB interaction as a result of LP2 → $\sigma^*(O_d$—$H_1)$ charge transfer, within the NBO framework in all the studied cases, Fig. 6. A comprehensive summary of the NBO results is presented in Table 5 corresponding to the ground state optimized geometries of the studied molecules. The occupation numbers of both the lone pair orbitals (LP1 and LP2) are found to bear reasonable harmony with other NBO results as discussed above. The data compiled in Table 5 also surprisingly highlight that the LP2 → $\sigma^*(O_d$—$H_1)$ hyperconjugative charge transfer stabilization energy (ΔE_2) is almost independent of the electronegativity of the 5-halo group.

In an X—H···Y hydrogen bonding system, a repolarization of the X—H bond occur due to a shifting of the electron density and a concomitant rehybridization of the X atom takes place. These two effects in conjunction make the involved hydrogen atom more electropositive such that the 's' character of the X-hybrid atomic orbital of X—H bond increases leading to a bond contraction. Hyperconjugation and rehybridization thus act in opposite directions so that the net outcome (in terms of a red or blue-shift of the IR strech of X—H bond, for example) is governed by a balance

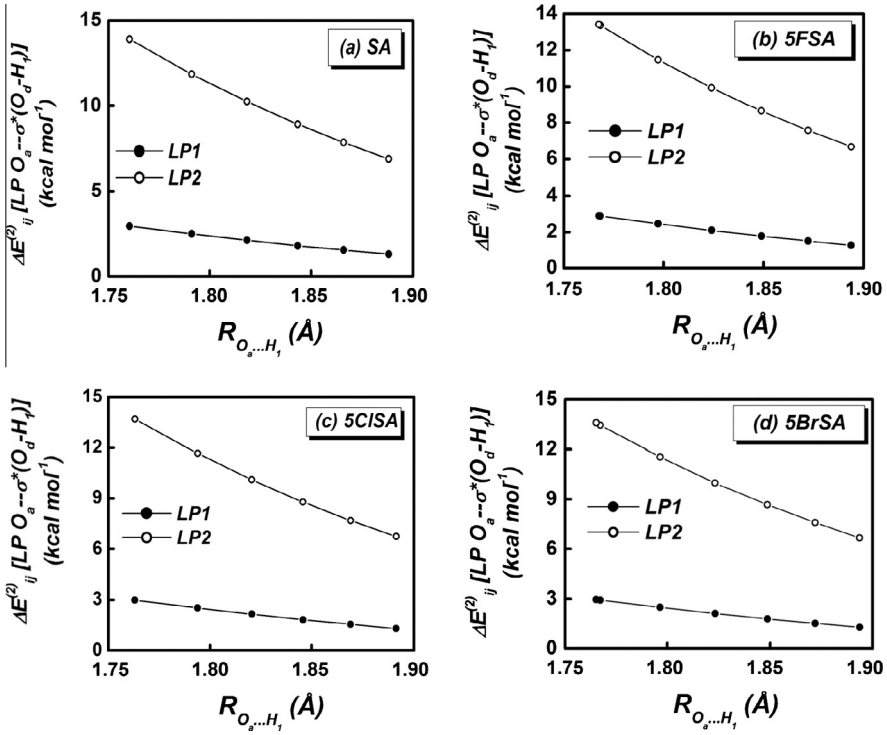

Fig. 4. Variation of hyperconjugative interaction energy ΔE_2 (LP(O_a) → $\sigma^*(O_d$—$H_1)$; LP1: –●– and LP2: –○–) as a function of the O_a···H_1 IMHB distance for the C-form of (a) SA, (b) 5FSA, (c) 5ClSA and (d) 5BrSA. The solid lines only provide a visual guide to the pattern of variation.

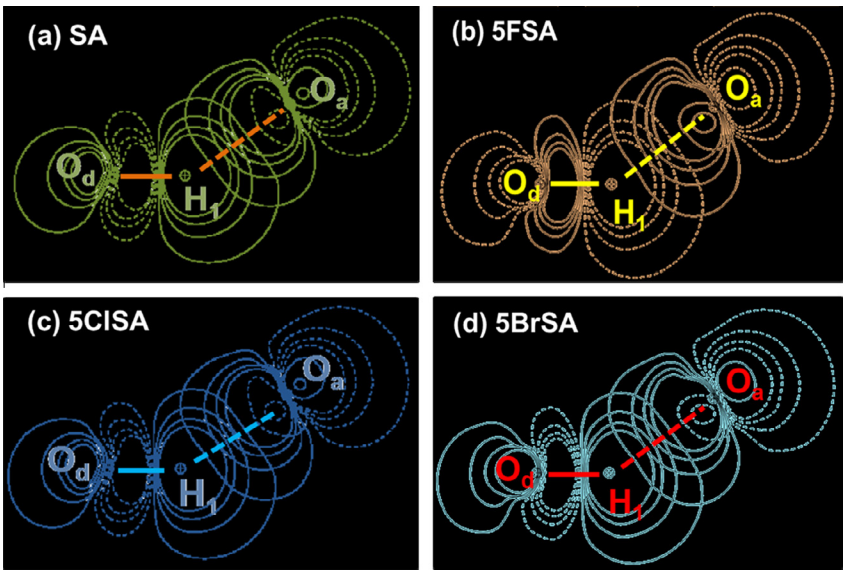

Fig. 5. Contour diagram showing the orbital (NBOs) interactions (LP Y → σ^*(X—H) hyperconjugative charge transfer interaction in X—H···Y hydrogen bond) involved in formation of the $O_a\cdots H_1$ IMHB in the C-form of (a) SA, (b) 5FSA, (c) 5ClSA and (d) 5BrSA. Overlap between the LP2 (O_a) and $\sigma O_d—H_1$) orbitals is shown.

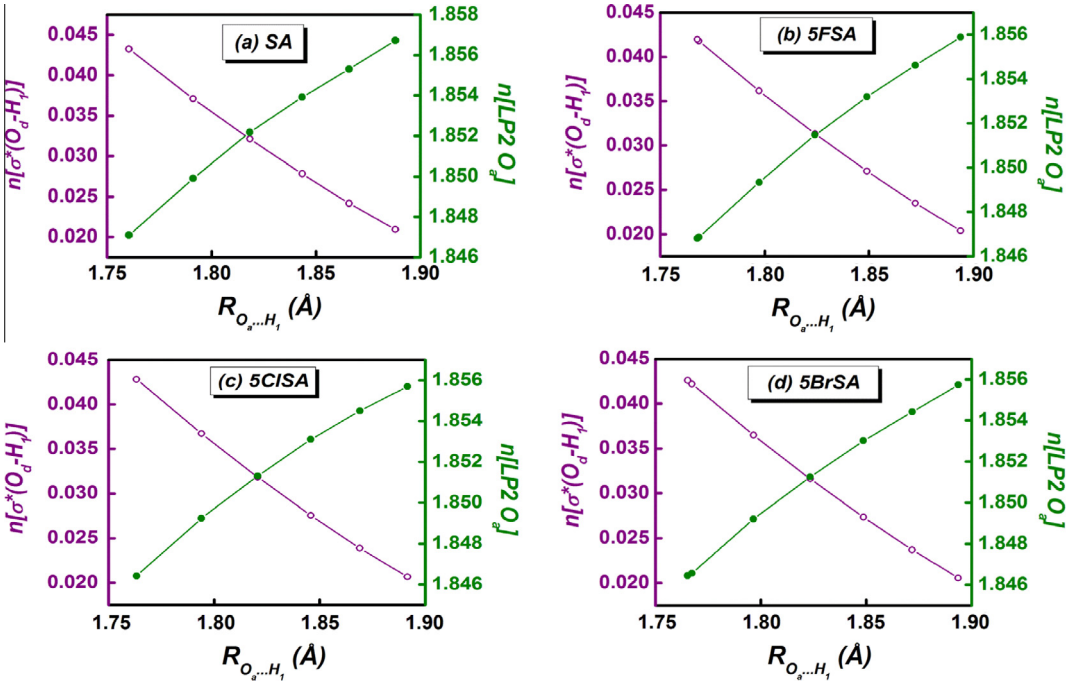

Fig. 6. Variation of NBO population in the orbitals LP2 O_a (–●–) and $\sigma^*(O_d—H_1)$ (–○–) of (a) SA, (b) 5FSA, (c) 5ClSA and (d) 5BrSA as a function of the $O_a\cdots H_1$ IMHB distance. The solid lines only provide a visual guide to the pattern of variation.

Table 5
Stabilization energies (ΔE_2) for selected NBO pairs as given by second-order perturbation theory analysis of the Fock matrix in the NBO basis for the intramolecularly hydrogen bonded C-form of the studied molecular systems as obtained from the B3LYP/6-311++G(d,p) calculations (atom numbering according to Scheme 1).

Molecule	Donor NBO, Φ_i	Acceptor NBO, Φ_j	ΔE_2 (kcal mol^{-1})	$\varepsilon_i-\varepsilon_j$ (a.u.)	F (a.u.)
SA	LP1 O_a	$\sigma^*(O_d—H_1)$	2.96	1.13	0.052
	LP2 O_a	$\sigma^*(O_d—H_1)$	13.90	0.72	0.092
5FSA	LP1 O_a	$\sigma^*(O_d—H_1)$	2.90	1.13	0.510
	LP2 O_a	$\sigma^*(O_d—H_1)$	13.40	0.72	0.090
5ClSA	LP1 O_a	$\sigma^*(O_d—H_1)$	2.97	1.13	0.052
	LP2 O_a	$\sigma^*(O_d—H_1)$	13.70	0.71	0.091
5BrSA	LP1 O_a	$\sigma^*(O_d—H_1)$	2.95	1.13	0.052
	LP2 O_a	$\sigma^*(O_d—H_1)$	13.58	0.71	0.090

of the two effects. As obvious from Fig. 7, the variation of percentage s-character of O_d-centric hybrid atomic orbital of the O_d—H_1 bond in the studied molecular systems is found to attain the minimum value at the equilibrium geometry of the molecule in all cases while it increases with elongation of the O_a···H_1 distance. This result strongly substantiates the instrumental role of hyperconjugation rather than rehybridization in the studied IMHB systems which thereby leads to a blue-shift in IR stretch for the O_d—H_1 bond on moving from the C-form to the O-form (see Section 3.2, *vide* Table 2) [16,17,31,53].

3.5. Interplay between IMHB and aromaticity

The concept of Resonance-Assisted Hydrogen Bonds (RAHBs) was coined by Gilli and coworkers [36]. Usually RAHBs are characterized by changes in geometrical or electronic properties, i.e., elongation of formal double bonds and shortening of formal single bonds, together with elongation of the X—H bond and shortening of the H···Y bond within the H-bridge: X—H···Y [16,31,36]. The comparison of optimized geometry parameters between the closed and open conformations of the studied molecular systems (*vide* Section 3.1, Table 1) led to the initial indications for the occurrence of RAHB in the systems (*cf.* Scheme 2). Herein, we make an effort to yield acumen into the interplay between the resonance assistance in the IMHB interaction and the aromaticity of the benzene nucleus. The descriptors of aromaticity used in the work and relevant discussions regarding their calculations are presented in Section 2.3 and the results are compiled in Table 6.

Three simultaneous π-electron delocalization effects can be considered within the analyzed systems. The first one refers to the global π-electron delocalization effect occurring within the aromatic nucleus, leading to stabilization of the species. According to Clar's model [67–69], an aromatic π-sextet in a Kekulé resonance structure is defined as six π-electrons localized in a single

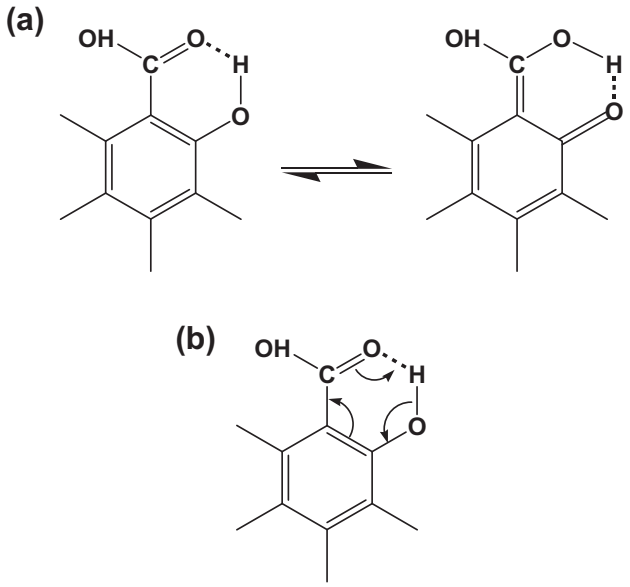

Scheme 2. Schematic paradigm for (a) IMHB interaction between the aromatic ring and the substituents in the corresponding tautomeric forms, (b) electronic movement in the cyclic resonance-assisted hydrogen bonding interaction involving the benzene aromatic nucleus.

Table 6
Comparison of different aromaticity indices (closed form vs. open form) for SA, 5FSA, 5ClSA, and 5BrSA.

Molecule	HOMA	NICS(0)	NICS(1)
SA	0.928 vs. 0.953	−7.994 vs. −8.740	−9.104 vs. −9.542
5FSA	0.929 vs. 0.953	−9.956 vs. −10.669	−9.399 vs. −9.768
5ClSA	0.932 vs. 0.957	−8.792 vs. −9.339	−8.919 vs. −9.261
5BrSA	0.932 vs. 0.956	−8.631 vs. −9.274	−8.976 vs. −9.254

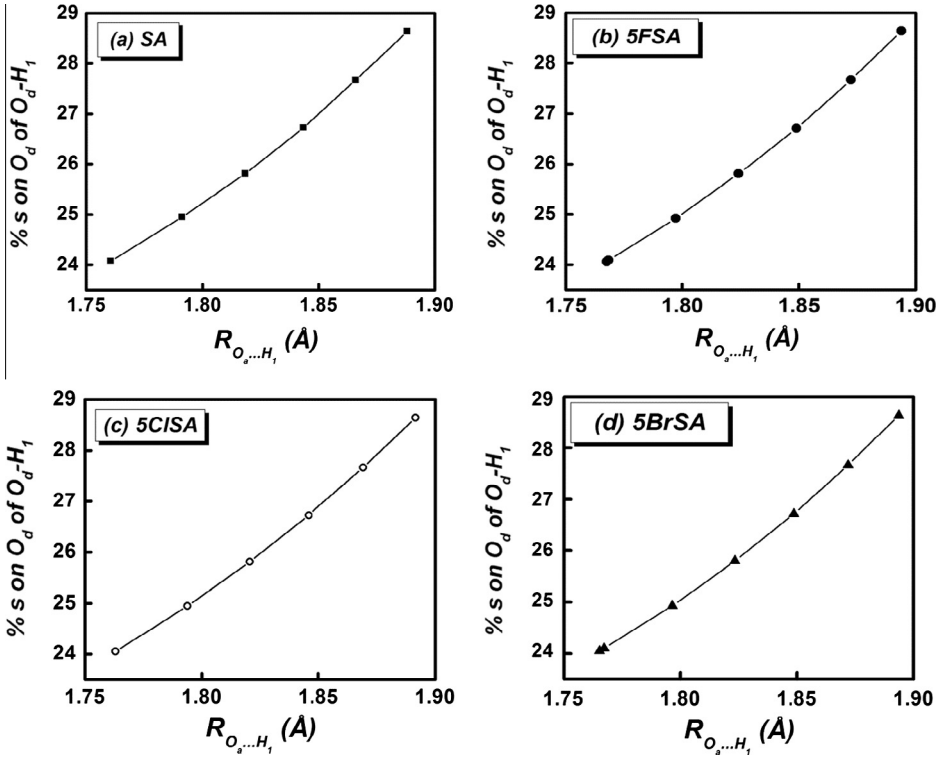

Fig. 7. Variation of the percentage 's'-character in O_d-centric hybrid orbital of the $\sigma(O_d—H_1)$ bond of (a) SA (–■–), (b) 5FSA (–●–), (c) 5ClSA (–○–) and (d) 5BrSA (–▲–) as a function of the O_a···H_1 IMHB distance. The solid lines only provide a visual guide to the pattern of variation.

benzene ring separated from adjacent rings by formal CC single bonds. Thus, this model refers to the Kekulé resonance structure with the largest number of disjoint aromatic π-sextets to be the Clar structure [31,67]. However, our investigated systems are devoid of such additional complexities by the presence of only one ring in the molecule and the π-sextet of electrons is thus localized within that ring.

The second effect is concerned about the interaction between the substituents present in the aromatic ring. A schematic of the effect is shown in a general manner for all the studied molecules in Scheme 2. It is obvious that the communication between substituents (Mesomeric effect) engages the π-electrons of the aromatic nucleus. It is thus conventionally argued that the effect of interaction between the substituents proceeds in a direction that resists the process of π-electron delocalization within the ring, whereby perturbing the uniform electronic distribution within the aromatic ring [16,31,70]. Therefore, the global π-electron delocalization effect and the effect of substituents are mutually competitive. The operation of the substituent effect should thus lead to a decrement of the aromaticity of the ring compared to the unsubstituted counterpart. Indeed, all aromaticity indices used in this work are found to substantiate this postulation through a comparison between the closed and open forms of all the studied systems (*cf.* Table 6). Therefore, it is logical at this stage to argue that the mutually competitive global π-electron delocalization effect and the substituent effect are present in all the investigated systems and the IMHB interaction plays a role in determining the local aromaticity of the systems. In fact, the last effect to be discussed in the series is strictly associated with the intramolecular RAHB and is applicable to closed conformations only. As is evident from Scheme 2, the effect of resonance within the additional quasi-aromatic ring formed from the RAHB interaction proceeds in the same direction as it is for the substituent effect (*cf.* Scheme 2). Therefore, these two effects should mutually cooperate. Even it is postulated by some authors that both the effect of communication between the substituents and the resonance accompanying H-bonding are in fact the same phenomenon which can be considered as an amplified mesomeric effect where the amplification is due to the formation of the extra quasi-aromatic ring [31,68,70]. These results corroborating to the formation of RAHB in the studied molecular systems probably points out that determination of IMHB energy simply by calculating the energy difference between the intramolecularly hydrogen bonded closed form (C-form) and the non-hydrogen bonded open form is not a rational method to apply (it may even be misleading), at least for the presently investigated molecules and within the present computational window. A basic pitfall of

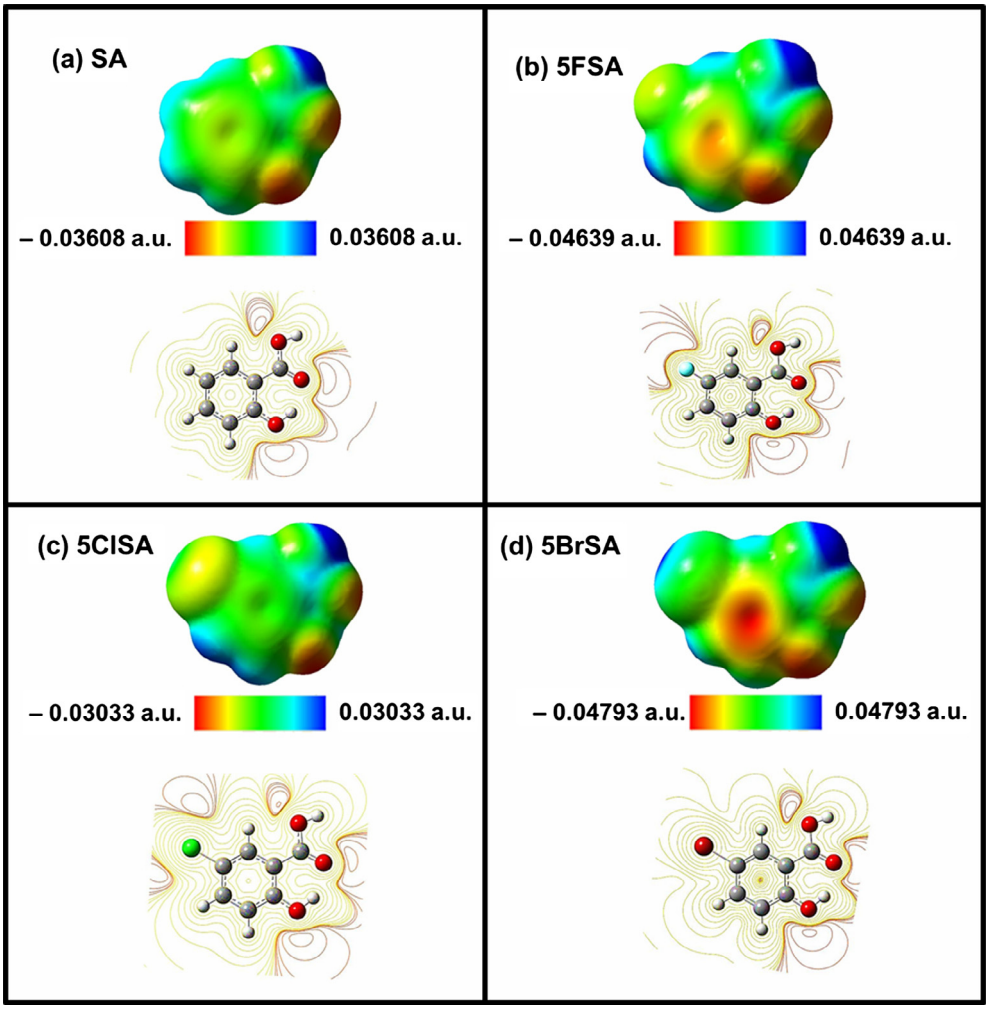

Fig. 8. The total electron density isosurface mapped with molecular electrostatic potential (MEP) of (a) SA, (b) 5FSA, (c) 5ClSA and (d) 5BrSA. Isovalue = 0.0004. Level of calculation: B3LYP/6-311++G(d,p). The color scheme for the MEPS is as follows: red – electron rich, partially negative charge; yellow – slightly electron rich region; blue – electron deficient, partially positive charge; light blue – slightly electron deficient region; green – neutral. On the lower panels are displayed the contour maps of the molecular electrostatic potential surface (MEPS) over the optimized geometries of the respective molecular systems. (For interpretation of the references to color in this figure legend, the reader is referred to the web version of this article.)

this method may creep in the assumption of ignoring the interactions of the lone pair electrons on the oxygen atom of the —OH functional moiety with the π-electron system of the aromatic nucleus via C_2=C_3 bond which could be manifested as resonance interaction energy differences. This apparently simple strategy also ignores other geometry parameters and their subsequent effect on the molecular optimized energies during rotation of the O_d—H_1 functional moiety to produce the non-hydrogen bonded open conformer [71].

3.6. Molecular electrostatic potential surface (MEPS)

The molecular electrostatic potential surface (MEPS) is a method of mapping electrostatic potential onto the isoelectron density surface which in turn enables a simultaneous display of the distribution of electrostatic potential (electrons + nuclei), shape, size and dipole moments of the molecule. Consequently, it can be used as a useful descriptor for identifying sites for hydrogen bonding interactions. Atomic charges cannot in general be defined uniquely, and it is actually the electrostatic field around a molecule that is more directly relevant to the recognition of molecular properties. This justifies the usefulness of a three-dimensional electrostatic potential map encompassing the entire molecule as a reliable descriptor of hydrogen bonding interaction which is largely an electrostatic phenomenon [31,72–74].

Isoelectronic molecular electrostatic potential surfaces (MEPS) and electron density surfaces [72–74] were calculated at B3LYP/6-311++G(d,p) level. The molecular electrostatic potential (MEP) at a point $r(x,y,z)$ in the space around a molecule (in atomic units) is defined in terms of the interaction energy between the electrical charge generated from the molecule's electrons and nuclei and a positive test charge (a proton) located at **r** and can be expressed as:

$$V(\mathbf{r}) = \sum_A \frac{Z_A}{|\vec{R_A} - \vec{\mathbf{r}}|} - \int \frac{\rho(\vec{\mathbf{r}'})d\mathbf{r}'}{|\vec{\mathbf{r}'} - \vec{\mathbf{r}}|} \quad (8)$$

where Z_A is the charge on nucleus A, located at R_A, $\rho(\mathbf{r}')$ is the electronic density function for the molecule and $\mathbf{r}'$ is the dummy integration variable. The first and second terms represent the contributions to the potential due to nuclei and electrons, respectively. $V(\mathbf{r})$ is the resultant at each point **r**, which is the net electrostatic effect produced at the point **r** by both the electrons and nuclei of the molecule. An additional edge of the electrostatic potential is that it is a real physical property, which can be determined both experimentally, by diffraction methods, as well as computationally [73,74]. The total electron density surface mapped with the electrostatic potential and the corresponding contours of the studied molecules are displayed in Fig. 8. In course of studying the possible correlation of electrostatic potential with hydrogen bonding interaction, the regions of negative electrostatic potential (denoted by red) are usually used to identify hydrogen bond acceptor sites, while for describing the hydrogen bond donating sites the regions of positive potential (denoted by blue) are highlighted. Fig. 8 clearly reflects a negative potential on O_a-atom (reddish) and thereby justifies its ability to function as an H-bond acceptor site, which is further validated from a closer scrutiny of the contour diagrams. The positive electrostatic potential on the H_1-atom follows the same line of argument and hence substantiates the occurrence of IMHB interaction in the molecular systems under study.

4. Discussion and conclusions

The present work describes a quantum chemical investigation to explore the intramolecular hydrogen bond (IMHB) interaction in salicylic acid (SA) and its 5-halo derivatives *viz.*, 5FSA, 5ClSA and 5BrSA. The IMHB interaction has been addressed from various computational strategies e.g., geometric criteria, computational spectroscopy (simulated IR spectra), topological analysis based on AIM theory, population analysis based on NBO technique, aromaticity analysis of the benzene nucleus in the context of RAHB concept, and the molecular electrostatic potential surface. All the computational strategies explicitly establish the presence of IMHB in the studied molecular systems while the directional nature of the interaction is unveiled under the NBO provision.

It is also noted that none of the aforesaid techniques reveal a definite pattern or correlation between the IMHB energy and the electronergativity of the 5-halo substituent in the molecules under analysis. In this context it is thus concluded that the electronergativity of the 5-halo substituent might not be the sole factor governing the IMHB energy in the studied molecular systems. A conjugate impact of electron withdrawing inductive and electron donating resonance effects of the halogen atoms might play the key role in governing the overall findings.

At this stage, it is intriguing to note that quantum chemical description yields more consensus picture of the IMHB interaction with different findings [28–31,75] as against the geometry criteria. The topological parameters provided by AIM theory are calculated with $\rho(\mathbf{r})$ on the optimized geometries for a series of hydrogen bond distances. The variation of these properties with these distances paves way for analyzing the nature of the interaction within the X—H···Y hydrogen bond framework. At large IMHB distances the electrostatic attraction predominates, while the quantum effects associated with redistribution of $\rho(\mathbf{r})$ around H and Y atoms dominate the interaction in the vicinity of the equilibrium geometry [71]. Although the range of distances included typically displays noncovalent bond features, showing signatures of covalent interactions beginning to appear in the neighborhood of equilibrium geometry. This is prudently conjoined with a picture of resonance assistance in the IMHB interaction and is aptly substantiated from the interplay between IMHB energy and aromaticity in which both geometric and magnetic descriptors of aromaticity produce consistent results.

In conclusion it can be stated that the present study articulates the presence of IMHB interaction in the lowest energy ground state conformers of all the molecular systems under investigation, however, with a conspicuous lack of a correlation between the electronegativity of the 5-halo substituent and the IMHB energy. Such observation possibly indicates at the complex interplay between the electron attracting inductive and electron donating resonance effects of the substituent atoms and their differential influences on the IMHB forming functional moieties. More importantly to note is the inadequacy of the geometrical criteria while on contrary, the accuracy of the quantum chemical treatment to illuminate the deeper aspects of H-Bonding interaction. Furthermore, some important properties of the IMHB interactions in the studied molecules e.g., directional nature, presence of partial covalency are fruitfully assessed from the quantum chemical parameters. The nature of the interaction and its evolution with varying IMHB distances for all the molecular systems are also found to be more accurately described from the quantum chemical perspectives.

Acknowledgements

A.G. and S.G. gratefully acknowledge Junior Research Fellowships respectively from CSIR and UGC, New Delhi, Govt. of India. N.G. likes to acknowledge UPE and CRNN, CU, CSIR, India and DST, India for funding.

References

[1] G.R. Desiraju, T. Steiner, The Weak Hydrogen Bond: In Structural Chemistry and Biology, Oxford University Press, Oxford, 1999.

[2] S. Scheiner, Hydrogen Bonding: A Theoretical Perspective, Oxford University Press, New York, 1997.
[3] I. Alkorta, I. Rozas, J. Elguero, Non-conventional hydrogen bonds, Chem. Soc. Rev. 27 (1998) 163–170.
[4] L. Sobczyk, S.J. Grabowski, T.M. Krygowski, Interrelation between H-Bond and Pi-Electron Delocalization, Chem. Rev. 105 (2005) 3513–3560.
[5] G.R. Desiraju, Reflections on the hydrogen bond in crystal engineering, Cryst. Growth Des. 11 (2011) 896–898.
[6] F. Franks (Ed.), Water. A Comprehensive Treatise, Plenum Press, New York, 1972.
[7] G.R. Desiraju, Crystal engineering: a holistic view, Angew. Chem. Int. Ed. 46 (2007) 8342–8356.
[8] S.J. Grabowski, What is the covalency of hydrogen bonding?, Chem Rev. 111 (2011) 2597–2625.
[9] G.R. Desiraju, A bond by any other name, Angew. Chem. Int. Ed. 50 (2011) 52–59.
[10] E. Arunan, G.R. Desiraju, R.A. Klein, J. Sadlej, S. Scheiner, I. Alkorta, D.C. Clary, R.H. Crabtree, J.J. Dannenberg, P. Hobza, H.G. Kjaergaard, A.C. Legon, B. Mennucci, D.J. Nesbitt, Definition of the hydrogen bond (IUPAC Recommendations 2011), Pure Appl. Chem. 82 (2010) 1637–1641.
[11] C.G. Cannon, The nature of hydrogen bonding, Spectrochim. Acta 10 (1958) 341–368.
[12] I.G. Kaplan, Theory of Molecular Interactions; Studies in Physical and Theoretical Chemistry, vol. 42, Elsevier, Amsterdam, The Netherlands, 1986.
[13] S.J. Grabowski, Ab initio calculations on conventional and unconventional hydrogen bonds−study of the hydrogen bond strength, J. Phys. Chem. A 105 (2001) 10739–10746.
[14] G.R. Desiraju, Hydrogen bridges in crystal engineering: interactions without borders, Acc. Chem. Res. 35 (2002) 565–573.
[15] L.G. Arnaut, S.J. Formosinho, Excited-state proton transfer reactions I. Fundamentals and intermolecular reactions, J. Photochem. Photobiol. A 75 (1993) 1–20.
[16] S. Mahanta, B.K. Paul, R.B. Singh, N. Guchhait, Inequivalence of substitution pairs in hydroxynaphthaldehyde: a theoretical measurement by intramolecular hydrogen bond strength, aromaticity, and excited-state intramolecular proton transfer reaction, J. Comput. Chem. 32 (2011) 1–14.
[17] B.K. Paul, S. Mahanta, R.B. Singh, N. Guchhait, A DFT-based theoretical study on the photophysics of 4-hydroxyacridine: single-water-mediated excited state proton transfer, J. Phys. Chem. A 114 (2010) 2618–2627.
[18] A.H. Weller, Intramolecular proton transfer in excited states, Z. Elektrochem. 60 (1956) 1144–1147.
[19] B.K. Paul, A. Samanta, N. Guchhait, Modulation of excited-state intramolecular proton transfer reaction of 1-hydroxy-2-naphthaldehyde in different supramolecular assemblies, Langmuir 26 (2010) 3214–3224.
[20] B.K. Paul, N. Guchhait, Modulation of prototropic activity and rotational Relaxation dynamics of a cationic biological photosensitizer within the motionally constrained bio-environment of a protein, J. Phys. Chem. B 115 (2011) 10322–10334.
[21] J. Catalan, J.C. del Valle, R.M. Claramunt, D. Sanz, J. Dotor, Photophysics of the 2-(2′-hydroxyphenyl)perimidine: on the fluorescence of the enol form, J. Lumin. 68 (1996) 165–170.
[22] M.E. Balmer, H.-R. Buser, M.D. Muller, T. Poiger, Occurrence of some organic UV filters in wastewater, in surface waters, and in fish from Swiss Lakes, Environ. Sci. Technol. 39 (2005) 953–962.
[23] L.A. Helmbrook, J.E. Kenny, B.E. Kohler, G.W. Scott, Lowest excited singlet state of hydrogen-bonded methyl salicylate, J. Phys. Chem. 87 (1983) 280–289.
[24] F. Lahmani, A. Zehnacker-Rentien, Effect of substitution on the photoinduced intramolecular proton transfer in salicylic acid, J. Phys. Chem. A 101 (1997) 6141–6147. and references therein.
[25] L. Rodriguez-Santiago, M. Sodupe, A. Oliva, J. Bertran, Hydrogen atom or proton transfer in neutral and single positive ions of salicylic acid and related compounds, J. Am. Chem. Soc. 121 (1999) 8882–8890.
[26] H.C. Joshi, C. Gooijer, G. van der Zwan, Substitution effects on the photophysical characteristics of the salicylic anion, J. Fluoresc. 13 (2003) 227–234.
[27] I.P. Pozdnyakov, A. Pigliucci, N. Tkachenko, V.F. Plyusnin, E. Vauthey, H. Lemmetyinen, The photophysics of salicylic acid derivatives in aqueous solution, J. Phys. Org. Chem. 22 (2009) 449–454.
[28] B.K. Paul, A. Samanta, N. Guchhait, Deciphering the photophysics of 5-chlorosalicylic acid: evidence for excited-state intramolecular proton transfer, Photochem. Photobiol. Sci. 9 (2010) 57–67.
[29] B.K. Paul, A. Samanta, N. Guchhait, Influence of chlorine substitution on intramolecular hydrogen bond energy and ESIPT barrier: experimental and theoretical measurements on the photophysics of 3,5-dichlorosalicylic acid, J. Mol. Struct. 977 (2010) 78–89.
[30] B.K. Paul, A. Samanta, N. Guchhait, On the photophysics of 3,5,6-trichlorosalicylic acid: spectroscopic study combined with Hartree-Fock and density functional theory calculations, J. Fluoresc. 21 (2011) 1265–1279.
[31] B.K. Paul, N. Guchhait, Geometrical criteria versus quantum chemical criteria for assessment of intramolecular hydrogen bond (IMHB) interaction: a computational comparison into the effect of chlorine substitution on IMHB of salicylic acid in its lowest energy ground state conformer, Chem. Phys. 412 (2013) 58–67.
[32] R.F.W. Bader, Atoms in Molecules, A Quantum Theory, Clarendon Press, Oxford, U. K., 2000.
[33] P. Hobza, Z. Havlas, Blue-shifting hydrogen bonds, Chem. Rev. 100 (2000) 4253–4264.
[34] E.D. Glendening, A.E. Reed, J.E. Carpenter, F.A. Weinhold, NBO, Version 3.1, 1995.
[35] A.E. Reed, L.A. Curtiss, F.A. Weinhold, Intermolecular interactions from a natural bond orbital, donor-acceptor viewpoint, Chem. Rev. 88 (1988) 899–926.
[36] G. Gilli, V. Bertolasi, in: Z. Rappoport (Ed.), The Chemistry of Enols, Wiley, Chichester, U.K., 1990. Chapter 13.
[37] M.J. Frisch, G.W. Trucks, H.B. Schlegel, G.E. Scuseria, M.A. Robb, J.R. Cheeseman, J.A. Montgomery Jr., T. Vreven, K.N. Kudin, J.C. Burant, J.M. Millam, S.S. Iyengar, J. Tomasi, V. Barone, B. Mennucci, M. Cossi, G. Scalmani, N. Rega, G.A. Petersson, H. Nakatsuji, M. Hada, M. Ehara, K. Toyota, R. Fukuda, J. Hasegawa, M. Ishida, T. Nakajima, Y. Honda, O. Kitao, H. Nakai, M. Klene, X. Li, J.E. Knox, H.P. Hratchian, J.B. Cross, C. Adamo, J. Jaramillo, R. Gomperts, R.E. Stratmann, O. Yazyev, A.J. Austin, R. Cammi, C. Pomelli, J.W. Ochterski, P.Y. Ayala, K. Morokuma, G.A. Voth, P. Salvador, J.J. Dannenberg, V.G. Zakrzewski, S. Dapprich, A.D. Daniels, M.C. Strain, O. Farkas, D.K. Malick, A.D. Rabuck, K. Raghavachari, J.B. Foresman, J.V. Ortiz, Q. Cui, A.G. Baboul, S. Clifford, J. Cioslowski, B.B. Stefanov, G. Liu, A. Liashenko, P. Piskorz, I. Komaromi, R.L. Martin, D.J. Fox, T. Keith, M.A. Al-Laham, C.Y. Peng, A. Nanayakkara, M. Challacombe, P.M.W. Gill, B. Johnson, W. Chen, M.W. Wong, C. Gonzalez, J.A. Pople, Gaussian 03, Revision B.03, Gaussian, Inc., Pittsburgh, PA, 2003.
[38] W. Kohn, L. Sham, Self-consistent equations including exchange and correlation effects, Phys. Rev. 140 (1965) A1133–A1138.
[39] A.D. Becke, Density-functional thermochemistry. III. The role of exact exchange, J. Chem. Phys. 98 (1993) 5648–5652.
[40] C. Lee, W. Yang, R.G. Parr, Development of the Colle-Salvetti correlation-energy formula into a functional of the electron density, Phys. Rev. B 37 (1988) 785–789.
[41] T. Clark, J. Chandrasekhar, G.W. Spitznagel, P.v.R. Schleyer, Efficient diffuse function-augmented basis sets for anion calculations. III. The 3–21+G basis set for first-row elements, Li–F, J. Comput. Chem. 4 (1983) 294–301.
[42] J. Kruszewski, T.M. Krygowski, Definition of aromaticity basing on the harmonic oscillator model, Tetrahedron Lett. 13 (1972) 3839–3842.
[43] P.v.R. Schleyer, C. Maerker, A. Dransfeld, H. Jiao, N.J.R. Hommes, Nucleus-independent chemical shifts: a simple and efficient aromaticity Probe, J. Am. Chem. Soc. 118 (1996) 6317–6318.
[44] H.F.B. Shaidaei, C.S. Wannere, C. Corminboeuf, R. Puchta, P.v.R. Schleyer, Which NICS aromaticity index for planar π rings is best?, Org Lett. 8 (2006) 863–866.
[45] P. Lazzeretti, Assessment of aromaticity via molecular response properties, Phys. Chem. Chem. Phys. 6 (2004) 217–223.
[46] J. Aihara, Nucleus-independent chemical shifts and local aromaticities in large polycyclic aromatic hydrocarbons, Chem. Phys. Lett. 365 (2002) 34–39.
[47] P. Schuster, in: P. Schuster, G. Zundel, C. Sandorfy (Eds.), The Hydrogen Bond, vol. I, North Holland, Amsterdam, The Netherlands, 1976.
[48] R.N. Musin, Y.H. Mariam, An integrated approach to the study of intramolecular hydrogen bonds in malonaldehyde enol derivatives and naphthazarin: trend in energetic versus geometrical consequences, J. Phys. Org. Chem. 19 (2006) 425–444.
[49] M. Jablonski, A. Kaczmarek, A.J. Sadlej, Estimates of the energy of intramolecular hydrogen bonds, J. Phys. Chem. A 110 (2006) 10890–10898.
[50] E. Espinosa, E. Molins, Retrieving interaction potentials from the topology of the electron density distribution: the case of hydrogen bonds, J. Chem. Phys. 113 (2000) 5686–5694.
[51] M. Karabacak, E. Kosea, M. Kurt, FT-Raman, FT-IR spectra and DFT calculations on monomeric and dimeric structures of 5-fluoro- and 5-chloro-salicylic acid, J. Raman Spectrosc. 41 (2010) 1085–1097.
[52] M. Karabacak, M. Kurt, The spectroscopic (FT-IR and FT-Raman) and theoretical studies of 5-bromo-salicylic acid, J. Mol. Struct. 919 (2009) 215–222.
[53] B.K. Paul, N. Guchhait, A computational investigation on the intramolecular hydrogen bonding interaction and excited state intramolecular proton transfer process in 2-quinolin-2-yl-phenol, Comput. Theor. Chem. 978 (2011) 67–76.
[54] S.J. Grabowski, Hydrogen bonding strength—measures based on geometric and topological parameters, J. Phys. Org. Chem. 17 (2004) 18–31.
[55] U. Koch, P.L.A. Popelier, Characterization of C-H-O hydrogen bonds on the basis of the charge density, J. Phys. Chem. 99 (1995) 9747–9754.
[56] P.L.A. Popelier, Characterization of a dihydrogen bond on the basis of the electron density, J. Phys. Chem. A 102 (1998) 1873–1878.
[57] A. Mohajeri, F.F. Nobandegani, Detection and evaluation of hydrogen bond Strength in nucleic acid base pairs, J. Phys. Chem. A 112 (2008) 281–295.
[58] R.F.W. Bader, A bond path: a universal indicator of bonded interactions, J. Phys. Chem. A 102 (1998) 7314–7323.
[59] J. Cioslowski, S.T. Mixon, Topological properties of electron density in search of steric interactions in molecules: electronic structure calculations on ortho-substituted biphenyls, J. Am. Chem. Soc. 114 (1992) 4382–4387.
[60] J. Cioslowski, S.T. Mixon, E.D. Fleischmann, Electronic structures of trifluoro-, Tricyano-, and trinitromethane and their conjugate bases, J. Am. Chem. Soc. 113 (1991) 4751–4755.
[61] J. Poater, M. Sola, F.M. Bickelhaupt, Hydrogen–hydrogen bonding in planar biphenyl, predicted by Atoms-In-Molecules theory, does not exist, Chem. Eur. J. 12 (2006) 2889–2895.
[62] J. Poater, R. Visser, M. Sola, F.M. Bickelhaupt, Polycyclic benzenoids: why kinked is more stable than straight, J. Org. Chem. 72 (2007) 1134–1142.

[63] R.F.W. Bader, Bond paths are not chemical bonds, J. Phys. Chem. A 113 (2009) 10391–10396.
[64] S.J. Grabowski, J.M. Ugalde, Bond paths show preferable interactions: Ab initio and QTAIM studies on the X-H$\cdots\pi$ hydrogen bond, J. Phys. Chem. A 114 (2010) 7223–7229.
[65] S.J. Grabowski, Properties of a ring critical point as measures of intramolecular H-bond strength, Monatshefte für Chemie 133 (2002) 1373–1380.
[66] O. Galvez, P.C. Gomez, L.F. Pacios, Variation with the intermolecular distance of properties dependent on the electron density in hydrogen bond dimmers, J. Chem. Phys. 115 (2001) 11166–11183.
[67] E. Clar, In the Aromatic Sextet, Wiley, London, 1972.
[68] M. Randic, A.T. Balaban, Partitioning of π-electrons in rings for Clar structures of benzenoid hydrocarbons, J. Chem. Inf. Model. 46 (2006) 57–64.
[69] M. Randic, Aromaticity of polycyclic conjugated hydrocarbons, Chem. Rev. 103 (2003) 3449–3606.
[70] R. Kurczab, M.P. Mitoraj, A. Michalak, T. Ziegler, Theoretical analysis of the resonance assisted hydrogen bond based on the combined extended transition state method and natural orbitals for chemical valence scheme, J. Phys. Chem. A 114 (2010) 8581–8590.
[71] J.N. Woodford, Density functional theory and atoms-in-molecules investigation of intramolecular hydrogen bonding in derivatives of malonaldehyde and implications for resonance-assisted hydrogen bonding, J. Phys. Chem. A 111 (2007) 8519–8530.
[72] P.W. Kenny, Hydrogen bonding, electrostatic potential, and molecular design, J. Chem. Inf. Model. 49 (2009) 1234–1244.
[73] J.S. Murray, P. Politzer, Correlations between the solvent hydrogen-bond-donating parameter α and the calculated molecular surface electrostatic potential, J. Org. Chem. 56 (1991) 6715–6717.
[74] P. Politzer, D.G. Truhlar, EMS, Chemical Applications of Atomic and Molecular Electrostatic Potentials, Plenum Press, New York, 1981.
[75] S.J. Grabowski, An estimation of strength of intramolecular hydrogen bonds – *ab initio* and AIM studies, J. Mol. Struct. 562 (2001) 137–143.